possible effect of paramagnetic impurities upon the carbon-13 relaxation in solid poly(oxymethylene) can be ignored. Moreover, the observed carbon-13 relaxation (in particular, the effect of proton saturation) is typically as expected for proton–carbon dipolar relaxation.

Finally, we note that the observed $T_{1\rho}$ of the crystalline part (~2 ms) is shorter than the $T_{1\rho}$ of the amorphous part (~17.5 ms). This is not consistent with restricted molecular motions in the crystalline part, having correlation times comparable to the more isotropic motions occurring in the amorphous part. Instead, a longer $T_{1\rho}$ would be expected. This discrepancy results from the fact that the $T_{1\rho}$ of the crystalline carbons is determined by spin–spin interactions.[11,13] This is confirmed by proton $T_{1\rho}$ measurements in poly(oxymethylene)[26] in experiments where amorphous proton–crystalline proton spin diffusion has been reduced. The crystalline proton $T_{1\rho}$ then is 150 ms and the amorphous proton $T_{1\rho}$ is 30 ms; i.e., a longer (proton) $T_{1\rho}$ is observed for the crystalline part than for the amorphous part.

In conclusion, we feel that our data, combined with data from other experiments, suggest that molecular motions in solid poly(oxymethylene) take place in both amorphous and crystalline components and that these motions, possibly involving rotational oscillations of CH_2 units around the helical axis, can be characterized by (average) correlation times of the same order of magnitude. The amplitudes of these motions, however, are quite different, small-amplitude oscillations taking place in the crystalline component and larger amplitude motions in the amorphous components.

Obviously, measurement of carbon-13 spectra and relaxation parameters alone do not provide enough information to derive a clear model of the complex motions taking place in solid semicrystalline polymers. They do provide, however, useful complementary data, in particular, about the sites (or regions) where motions take place. In particular, carbon-13 line shapes and spin–lattice relaxation times in the laboratory frame seem to be useful parameters in the study of molecular motions in solid polymers.

References and Notes

(1) *NMR: Basic Princ. Prog.* **1971**, *4*.
(2) Crist, B.; Peterlin, A. *J. Polym. Sci., Part A-2* **1971**, *9*, 557.
(3) Trappeniers, N. J.; Gerritsma, C. J.; Oosting, P. H. *Physica (Amsterdam)* **1964**, *30*, 997.
(4) Connor, T. M. *Trans. Faraday Soc.* **1964**, *60*, 1574.
(5) Axelson, D. E.; Mandelkern, L. *ACS Symp. Ser.* **1979**, *No. 103*, 181.
(6) Pines, A.; Gibby, M. G.; Waugh, J. S. *J. Chem. Phys.* **1973**, *59*, 569.
(7) Andrew, E. R. *Prog. NMR Spectrosc.* **1971**, *8*, 1.
(8) Schaefer, J.; Stejskal, E. O. *J. Am. Chem. Soc.* **1976**, *98*, 1031.
(9) Schaefer, J.; Stejskal, E. O.; Buchdahl, R. *Macromolecules* **1977**, *10*, 384.
(10) Veeman, W. S.; Menger, E. M.; Ritchey, W.; de Boer, E. *Macromolecules* **1979**, *12*, 924.
(11) Stejskal, E. O.; Schaefer, J.; Steger, T. R. *Symp. Faraday Soc.* **1979**, *13*, 56.
(12) Garroway, A. N.; Moniz, W. B.; Resing, H. A. *Symp. Faraday Soc.* **1979**, *13*, 63.
(13) VanderHart, D. L.; Garroway, A. N. *J. Chem. Phys.* **1979**, *71*, 2773.
(14) Schaefer, J.; Stejskal, E. O.; Buchdahl, R. *Macromolecules* **1975**, *8*, 291.
(15) Earl, W. L.; VanderHart, D. L. *Macromolecules* **1979**, *12*, 762.
(16) VanderHart, D. L. *Macromolecules* **1979**, *12*, 1232.
(17) van Dijk, P. A. S.; Schut, W.; van Os, J. W. M.; Menger, E. M.; Veeman, W. S. *J. Phys. E* **1980**, *13*, 1309.
(18) Torchia, D. A. *J. Magn. Reson.* **1978**, *30*, 613.
(19) van Os, J. W. M.; Veeman, W. S. *Rev. Sci. Instrum.* **1979**, *50*, 445.
(20) Noggle, J. H.; Schirmer, R. E. "The Nuclear Overhauser Effect, Chemical Applications"; Academic Press: New York and London, 1971.
(21) Stejskal, E. O.; Schaefer, J.; Waugh, J. S. *J. Magn. Reson.* **1977**, *28*, 105.
(22) Shibata, T.; Iwayanagi, S. *Polym. J.* **1978**, *10*, 599.
(23) Odajima, A. *Suppl. Prog. Theor. Phys.* **1959**, *10*, 142.
(24) Schaefer, J. *Macromolecules* **1973**, *6*, 882.
(25) Ganapathy, S.; Naito, A.; McDowell, C. A. *J. Am. Chem. Soc.* **1981**, *103*, 6011.
(26) Veeman, W. S.; Menger, E. M. *Bull. Magn. Reson.* **1980**, *2*, 77.

Simulation Results for the End-to-End Vector Distribution Function of Short Polymethylene Chains

Ana M. Rubio and Juan J. Freire*

Departamento de Quimica Fisica, Facultad de Ciencias Quimicas, Universidad Complutense, Madrid-3, Spain.

Received January 29, 1982

ABSTRACT: Numerical results are obtained by means of simulation methods for the end-to-end vector distribution function of short polymethylene molecules represented by rotational isomeric chains and slightly different models. These results are used to test the accuracy of those previously obtained through quasi-analytical (i.e., nonsimulation) algorithms. Thus a procedure recently developed by Fixman et al. is confirmed to yield reasonably good values. The simulation results reveal orientational preferences in the region corresponding to small values of the end-to-end distance where intramolecular kinetic processes may occur when reactive groups are present. This region cannot be conveniently explored by current quasi-analytical methods.

I. Introduction

Correlations between the end repeating units of a polymer chain or, in general, between the terminal units of a sequence of N bonds along the polymer backbone have a fundamental role in the theory of dilute polymer solutions since they determine many macroscopic properties. These correlations are described by means of the end-to-end vector, $\mathbf{R}$, i.e., the vector joining the end units referred to a frame embedded in the sequence of bonds considered.[1] In many instances (polarized light scattering intensities, hydrodynamic properties, etc.) the macroscopic magnitudes depend mainly on the radial correlations[2] so that they can be conveniently related to the end-to-end distance, $R \equiv |\mathbf{R}|$. Some other properties (depolarized light scattering intensities,[3] change transfer between the ends of short chains,[4,5] etc.) depend on or may depend more strongly on the angular correlations. Thereby the end-to-end vector distribution function, $F(\mathbf{R})$, is a very interesting conformational characteristic of flexible-chain molecules.

For very long chains or sequences, i.e., for high values of N, $F(\mathbf{R})$ tends to be spherically symmetric and the

0024-9297/82/2215-1411$01.25/0

end-to-end distance distribution function, $F(R)$, is Gaussian. For shorter chains, however, the angular correlations are significant and, simultaneously, the radial dependence deviates from Gaussian behavior.[6] In these cases, numerical calculations for $F(\mathbf{R})$ become difficult.

Fixman et al.[7-9] have recently established a new method to obtain the end-to-end distance distribution function. The method is based on the inference of $F(R)$ from its even moments, $\langle R^{2p} \rangle$. They have also devised a new and more efficient algorithm[8,10] for the evaluation of these moments in order to extend the applicability of the inference. The results obtained with this method for the rotational isomeric representation of polymethylene chains[9] have been compared with Monte Carlo calculations previously reported by Yoon and Flory.[6] The agreement is excellent even for very short chains ($N = 10$), which indicates a high degree of accuracy of the quasi-analytical (i.e., nonsimulation) method.

The procedure has been extended[9,11] to the calculation of the end-to-end vector distribution function through an expansion of $F(\mathbf{R})$ in terms of the spherical harmonics corresponding to the angular spherical polar coordinates of $\mathbf{R}$. The radial-dependent coefficients of the expansion are inferred from some "generalized" moments[11] generated in the iterative calculation of even moments. The inference is performed by means of a second series expansion, now in terms of powers of R^2. As in the evaluation of $F(R)$, fluctuations of the rotational angles can be incorporated in a convenient way.

This double-expansion method has been applied to obtain $F(\mathbf{R})$ for short polymethylene chains[11] and the convergence of the results seems to be reasonably good. For the shortest chains, however, the values of $F(\mathbf{R})$ are considerably small in the region surrounding the first unit, where cyclization and intramolecular charge-transfer reactions occur when reactive groups are present. Then the convergence errors, though not important in absolute value, are significant enough to distort completely the information about orientation preferences in this zone.

In this work we evaluate $F(\mathbf{R})$ for the same chain model through simulation methods. We use a Monte Carlo method and a method based on an exhaustive enumeration of conformations. The latter procedure, which can only be applied to the shortest chains, serves to confirm the validity of the Monte Carlo calculations. According to the preceding paragraphs, the simulation results obtained for small values of R are the only reliable description of orientational preferences in this region. Moreover, results corresponding to higher values of R are needed to test the validity and accuracy of the quasi-analytical methods. We have also obtained simulation results for an extended model that includes intramolecular long-range interactions between the polymer units in order to ascertain the influence of these interactions on the distribution function.

In section II the simulation methods used in this work are described. The incorporation of fluctuations in the rotational angles and long-range interactions is explicitly detailed. Section III includes the exposition of results together with considerations related to their accuracy for the different methods and cases. These results are analyzed and discussed in section IV.

II. Numerical Methods

A. Generation of Conformations. In this work we have used two different simulation methods. The conformations are generated in both procedures as sequences of $N - 2$ rotational isomeric angles, $\{\phi_i\}$. The first method is based on a simple iteration that generates all the possible conformations by enumerating the different arrangements of rotational angles. Thus in order to obtain averages with this exhaustive enumeration method, the quantities of interest corresponding to a conformation should be weighted by a probability factor, p. For polymethylene chains, whose rotational angles are represented by three isomeric states (ϕ_i = t, g^+, g^-), p is evaluated as[7]

$$p = \frac{u(\phi_1)U(\phi_1,\phi_2)\ldots U(\phi_{N-3},\phi_{N-2})}{\mathbf{u}\mathbf{U}^{N-3}\mathbf{q}^t} \tag{1}$$

where

$$\mathbf{U} = \begin{pmatrix} 1 & \sigma & \sigma \\ 1 & \sigma & \sigma\omega \\ 1 & \sigma\omega & \sigma \end{pmatrix} \tag{2}$$

is the statistical weight matrix, indexed in the order t, g^+, g^-, $\mathbf{u}$ is the first row of $\mathbf{U}$, and $\mathbf{q} \equiv (1, 1, 1)$. Though the method is essentially exact for the model, it is useful only for very short chains with a total number of rotational isomeric conformations not too high. Thus simulations for relatively longer chains ($N \geq 14$) can only be accomplished by Monte Carlo methods.

Consequently, our second method is a Monte Carlo procedure. We obtain the sequence of rotational angles corresponding to a conformation by means of a subroutine that yields pseudorandom numbers within the range 0–1. To select a rotational angle ϕ_i, we divide this range into three regions whose amplitudes are proportional to the actual probabilities of the three possible rotational states along the sequence. The conditional probability that bond i is in state ϕ_i given that bond $i - 1$ is in state ϕ_{i-1} is[7]

$$f_i^c(\phi_{i-1}/\phi_i) = \frac{U(\phi_{i-1},\phi_i)[\mathbf{U}^{N-i-2}\mathbf{q}]_{\phi_i}}{[\mathbf{U}^{N-i-1}\mathbf{q}^t]_{\phi_{i-1}}} \tag{3}$$

where subscript ϕ_i denotes the ϕ_i'th element of the vector in brackets, indexed as matrix $\mathbf{U}$. For the first rotational angle the probability is

$$P(\phi_1) = \frac{u(\phi_i)[\mathbf{U}^{N-3}\mathbf{q}]_{\phi_i}}{\mathbf{u}\mathbf{U}^{N-3}\mathbf{q}^t} \tag{4}$$

Therefore the probability that a given conformation is generated corresponds in the Monte Carlo method to the actual global probability of this conformation, i.e., the product of conditional probabilities

$$p = P(\phi_1)f_2^c(\phi_1/\phi_2)\ldots f_{N-2}^c(\phi_{N-3}/\phi_{N-2}) \tag{5}$$

Consequently, the averages are evaluated directly as simple arithmetic means of the quantities obtained for different conformations so that in this method the values of p are not explicitly needed.

B. Model Modifications. The two simulation methods can be also applied to slightly different models. Thus we have considered for some cases independent Gaussian fluctuations in the rotational angles around their "rigid" values[9,12,13] with a given root-mean-square deviation, $\delta\phi$. The fluctuations are easily introduced in each conformation by extracting the rotational angles from sequences of Gaussianly distributed numbers with means corresponding to the previously chosen "rigid" values that characterize the conformation. Therefore we need to generate simultaneously three of these sequences for the three different values of the "rigid" rotational isomeric angles. The Gaussian sequences are obtained from samples of pseudorandom numbers.

Moreover, we have performed some calculations taking into account long-range interactions, i.e., interactions be-

tween units separated by more than four bonds along the chain. These interactions are represented by a hard-sphere potential[14] with a given distance of closest approach, d. The long-range interactions are not significant from the individual point of view so they can be treated by simplified potentials but they may affect the averaged dimensions of the chain in a collective way, giving rise to the excluded volume effect for long chains. In our simulations we consider the interactions by rejecting an initially chosen conformation if the distance between any pair of units separated by five or more bonds is smaller than d. The exhaustive enumeration method is slightly modified in these calculations so that the averages are now normalized respect to the sum of weight factors corresponding to the nonrejected conformations.

C. Calculation of Properties. Once a conformation is generated we obtain the coordinates of its $N + 1$ units. The initial coordinates are referred to the frame defined in previous works.[9,11] Thus the first unit is placed at the origin, the z axis points along the backbone bond vector $\mathbf{b}_1$ joining units 1 and 2, and the y axis points in the direction of $\mathbf{b}_1 \times \mathbf{b}_2$. Consequently, the coordinates of the second and third units are obtained according to the bond length, b (taken as unity in this work), and the bond angle, θ. The coordinates of successive units (x_i, y_i, z_i) are calculated from b, θ, the coordinates of the preceding three units along the chain, i.e., units $i - 3$, $i - 2$, and $i - 1$, and the rotational angle ϕ_{i-3}, which describes the rotation of bond $\mathbf{b}_{i-1}$ around bond $\mathbf{b}_{i-2}$. The coordinates of unit $N + 1$ are calculated this way. These coordinates, x, y, and z, define the end-to-end vector $\mathbf{R}$.

We record the values of x, y, and z and R^{2p} from p = 1–10 for each conformation. We obtain also the coordinates ρ_1, ρ_2, and ρ_3, which correspond to the conformation end-to-end vector in the reference frame defined by Yoon and Flory.[6] Axis ρ_1 was chosen by the latter authors to lie in our xz plane pointing along a direction close to that of the persistence vector $\langle \mathbf{R} \rangle$, an averaged vector that can be evaluated through accurate quasi-analytical methods.[6,9] Axis ρ_3 was located in the direction of our y axis. Finally, the origin of frame was placed at the end of the persistence vector. We divide the range of possible values for ρ_1, ρ_2, and ρ_3 into several intervals of equal length, $\Delta\rho$, so that each conformation is assigned to a cubic region which contains the coordinates of the end-to-end vector in this frame. Moreover, if the end-to-end distance of a given conformation is smaller than a certain value R_0, we also assign the conformation to the octant (defined by our initial frame) which contains the coordinates x, y, and z.

The averages $\langle x \rangle$, $\langle y \rangle$, $\langle z \rangle$, and $\langle R^{2p} \rangle$ and the numerical values of $F(\mathbf{R})$ are evaluated from sufficiently large samples of conformations. The latter quantities are obtained as averaged probability densities within different spatial regions. $F(\mathbf{R})$ is calculated in a specific region as the averaged number of conformations assigned to the region divided by its volume. Thus we obtain $F(\rho_1,\rho_2,\rho_3)$ from the number of conformations assigned to the cube whose center corresponds to these coordinates. Simultaneously, we obtain precise results for $F(\mathbf{R})$ around the point R = 0 from the number of conformations assigned to the different octants within a sphere of radius R_0 centered at this point.

III. Results

In this work we have made use of the rotational isomeric model parameters proposed by Flory[1,6] for polymethylene at 140 °C: $\theta = 68°$, $(t, g^+, g^-) = (0°, 120°, -120°)$, $\sigma = 0.54$, and $\omega = 0.088$. A value of 1.76 bond lengths[14] is adopted for the hard-sphere potential parameter d in the cases where long-range interactions are introduced.

We have calculated the averages $\langle x \rangle$, $\langle y \rangle$, $\langle z \rangle$, and $\langle R^{2p} \rangle$, from p = 1–10 for the rotational isomeric model with N = 10, 15, and 20 and $\delta\phi = 0°$ and 15°, i.e., without and with fluctuations in the rotational angles, by means of the Monte Carlo method. The results have been employed to test the accuracy of this method since the averages had been previously obtained by exact quasi-analytical algorithms.[6,9,12,13] Results obtained for $\delta\phi = 0°$ with the exhaustive enumeration method should be also exact. In fact, it is verified for N = 10 and $\delta\phi = 0°$ that differences between the numerical values extracted from these two types of exact procedures are extremely small (0.01% or smaller). The accuracy of the Monte Carlo results depends on the size of the statistical samples. We have used several samples (13 in most cases) for every chain or model. Each one of these samples contains 5×10^4 independent conformations and is characterized by a specific seed number which initiates the generation of pseudorandom values.

For each quantity, q, we have evaluated separately the averages corresponding to the different samples, q_i. Then the mean value of the averaged quantity, $\langle q \rangle$, is given by

$$\langle q \rangle = \sum_{i=1}^{n} q_i / n \tag{6}$$

where n is the number of samples. The error interval associated with the mean is estimated as Δq

$$\Delta q = \{\sum_{i=1}^{n} [q_i - \langle q_i \rangle]^2 / n(n-1)\}^{1/2} \tag{7}$$

We have verified that means and error intervals obtained from our samples for the different averages of coordinates are consistent with the exact quasi-analytic results for N = 10, 15, and 20 and $\delta\phi = 0°$ and 15°. The comparison between means and error intervals corresponding to the Monte Carlo end-to-end vector distribution functions with N = 10 and $\delta\phi = 0°$ and 15° and the exhaustive enumeration values is also satisfactory. All these facts ensure the validity of the Monte Carlo method.

The numerical values of $F(\rho_1,\rho_2,\rho_3)$ evaluated by simulation methods are sensitive to the interval length since the probability densities are averaged within regions whose volume is determined by $\Delta\rho$. This parameter should be chosen high enough to ensure smooth distributions that can be represented by continuous functions. Very high values of $\Delta\rho$ would, however, fade away the relevant physical information contained in the functions. The choice of $\Delta\rho$ is thereby conditioned by the number of possible conformations (referred to the simple rotational isomeric model) and the range of possible values of the end-to-end distance. Both factors are N dependent and they are predominant over more subtle characteristics of the model. For the values of N considered here, we have estimated that optimal intervals are defined with $\Delta\rho = (R_{max}/5)$, where R_{max} corresponds to the "all-trans" end-to-end distance

$$R_{max} = [\tfrac{1}{2}N^2(1 + \cos\theta) + (1 - \cos\theta)\sin^2(N\pi/2)]^{1/2} b \tag{8}$$

Consequently, the significant probability densities are averaged over 11^3 different cubic regions symmetrically disposed around the point $(\rho_1, \rho_2, \rho_3) = 0$.

Figures 1–3 show values of $F(\rho_1,\rho_2,\rho_3)$ for the rotational isomeric model with N = 10 and $\delta\phi = 0°$ and 15° along axes ρ_1, ρ_2, and ρ_3. The orientations of these axes ensure a well-defined behavior along them for reasonably smooth distribution functions. The values have been obtained with the exhaustive enumeration method so that they are practically exact. Figures 4–6 contain Monte Carlo results for N = 20 and $\delta\phi = 0°$ and 15°. The error interval of these values has been estimated to be about $\pm 2 \times 10^{-6}$ (bond

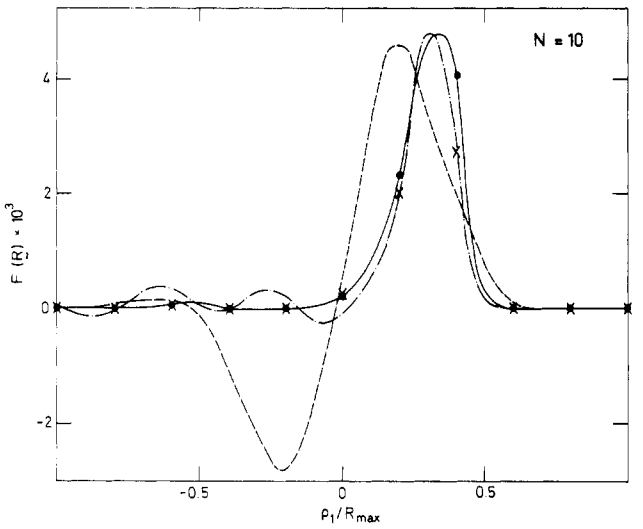

Figure 1. $F(\rho_1,0,0)$ in (bond lengths)$^{-3}$ for a polymethylene chain of 10 bonds at 140 °C: (●) simulation results for $\delta\phi = 0°$; (×) simulation results for $\delta\phi = 15°$; (–·–) double-expansion results;[11] (– – –) Yoon and Flory results.[6]

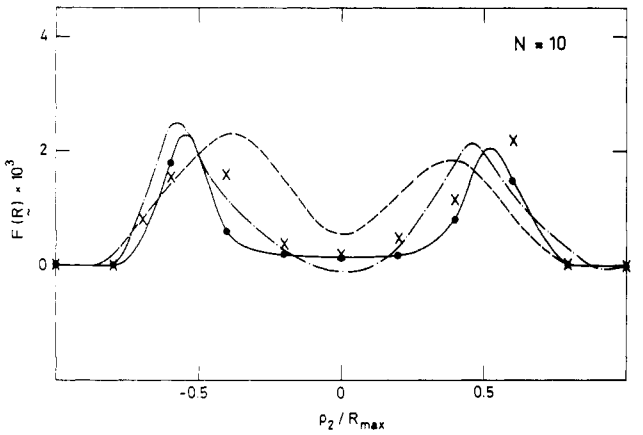

Figure 2. $F(0,\rho_2,0)$ for the $N = 10$ chain. See legend to Figure 1 for more details.

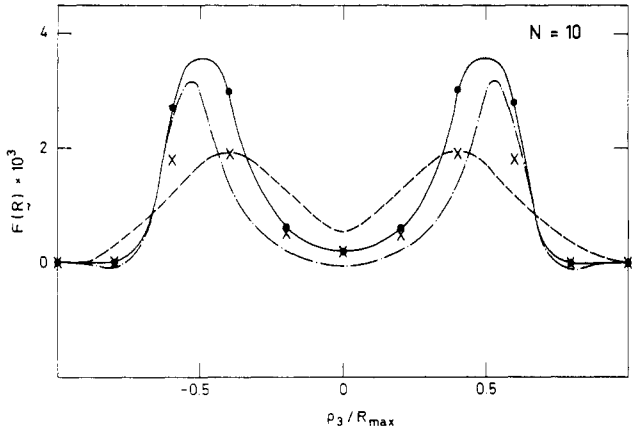

Figure 3. $F(0,0,\rho_3)$ for the $N = 10$ chain. See legend to Figure 1 for more details.

length)$^{-3}$. The numerical values for $\delta\phi = 0°$ have been joined in the figures by means of a solid line as an attempt to estimate the shape of a continuous distribution function.

Table I contains results for the probability density around the point $R = 0$ for $R_0 = 1$, 2, 4, and 5 bond lengths, with $N = 10$ and $\delta\phi = 0°$. These results have been obtained in different octants. The combinations of signs in the table denote the signs of coordinates x, y, and z in the corresponding octants. Results for $R_0 = 2$ bond lengths

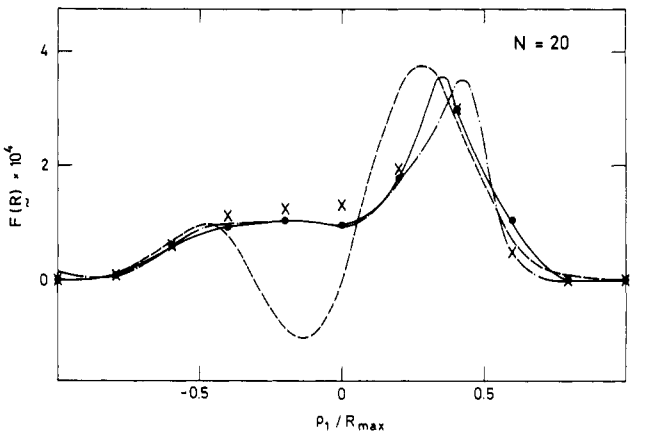

Figure 4. $F(\rho_1,0,0)$ for the $N = 20$ chain. See legend to Figure 1 for more details.

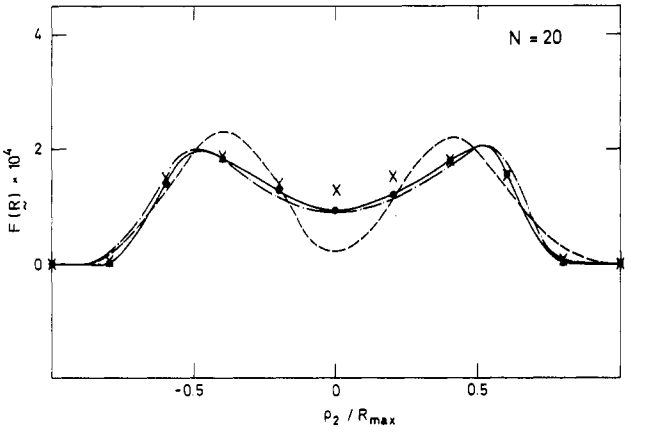

Figure 5. $F(0,\rho_2,0)$ for the $N = 20$ chain. See legend to Figure 1 for more details.

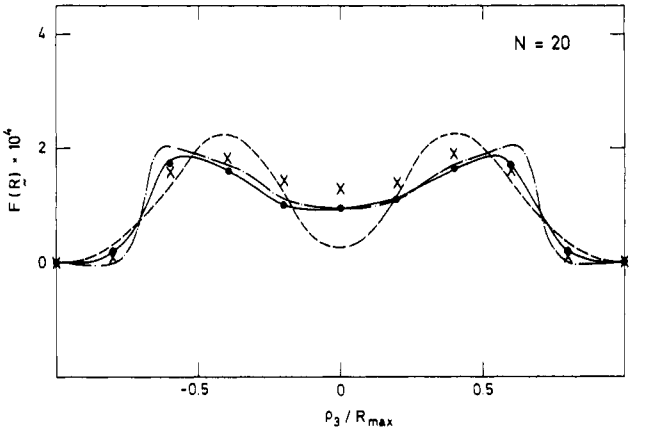

Figure 6. $F(0,0,\rho_3)$ for the $N = 20$ chain. See legend to Figure 1 for more details.

Table I
$10^5F(R)$ in (Bond Lengths)$^{-3}$ in Different Octants (Defined by Axes x, y, and z) of Spheres with Values of R_0 As Indicated (See Text) Obtained for Simple Polymethylene Chains with $N = 10$ and $\delta\phi = 0°$ at 140 °C

octant			R_0, bond lengths			
x	y	z	1	2	4	5
+	+	+	0.28	2.62	17.74	33.64
+	+	–	10.52	13.73	19.69	27.29
+	–	+	0.28	2.62	17.82	33.78
+	–	–	10.52	13.73	19.69	27.29
–	+	+	0.19	5.28	18.40	26.48
–	+	–	0.67	3.28	8.89	6.69
–	–	+	0.19	5.28	18.40	26.47
–	–	–	0.67	3.29	8.89	6.69

Table II
$10^5F(\mathbf{R})$ in (Bond Lengths)$^{-3}$ in Different Octants of a Sphere with $R_0 = 2$ Bond Lengths Obtained for Simple Polymethylene Chains at 140 °C with Values of N and $\delta\phi$ As Indicated

octant			$N = 10$	$N = 15$	$N = 15$	$N = 20$	$N = 20$
x	y	z	$\delta\phi = 15°$	$\delta\phi = 0°$	$\delta\phi = 15°$	$\delta\phi = 0°$	$\delta\phi = 15°$
+	+	+	3.5 ± 0.4	4.3 ± 0.5	10.0 ± 0.7	8.2 ± 0.7	13.1 ± 0.7
+	+	−	10.5 ± 0.7	8.5 ± 0.5	12.3 ± 0.7	12.8 ± 0.6	13.9 ± 0.6
+	−	+	3.0 ± 0.4	5.0 ± 0.8	9.4 ± 0.3	8.5 ± 0.5	13.4 ± 0.6
+	−	−	11.1 ± 0.5	8.7 ± 0.6	12.0 ± 1.0	14.1 ± 0.6	11.0 ± 0.6
−	+	+	5.3 ± 0.5	7.6 ± 0.3	11.8 ± 0.7	11.0 ± 0.4	12.2 ± 0.8
−	+	−	7.0 ± 0.5	6.1 ± 0.6	12.1 ± 0.6	14.3 ± 0.8	10.9 ± 0.8
−	−	+	5.8 ± 0.4	6.8 ± 0.5	12.1 ± 0.7	9.6 ± 0.6	12.6 ± 0.6
−	−	−	6.7 ± 0.5	5.5 ± 0.5	11.4 ± 0.7	12.9 ± 0.5	13.3 ± 0.4

Table III
$10^5F(\mathbf{R})$ in (Bond Lengths)$^{-3}$ in Different Octants of Spheres with Values of R_0 As Indicated Obtained for Simple Polymethylene Chains with $N = 10$ and $\delta\phi = 0°$ at 25 °C

octant			R_0, bond lengths		
x	y	z	1	2	4
+	+	+	0.02	0.69	9.44
+	+	−	2.03	4.42	11.33
+	−	+	0.02	0.69	9.44
+	−	−	2.03	4.42	11.33
−	+	+	0.01	1.07	11.04
−	+	−	0.04	0.67	4.72
−	−	+	0.01	1.07	11.04
−	−	−	0.04	0.69	4.72

Table IV
$10^5F(\mathbf{R})$ in (Bond Lengths)$^{-3}$ in Different Octants of Spheres with R_0 As Indicated Obtained for Polymethylene Chains with $N = 10$ and $\delta\phi = 0°$ at 140 °C Considering Intramolecular Long-Range Interactions

octant			R_0, bond lengths	
x	y	z	2	4
+	+	+	2.15	16.85
+	+	−	9.36	18.96
+	−	+	2.15	16.93
+	−	−	9.36	18.96
−	+	+	1.54	17.59
−	+	−	2.20	8.49
−	−	+	1.54	17.59
−	−	−	2.20	8.49

with different values of N and $\delta\phi$ are shown in Table II. For these cases the exhaustive enumeration has not been applied and, in consequence, the Monte Carlo results are presented together with their corresponding error intervals.

Some calculations have been also performed with statistical weight factors corresponding to a temperature of 25 °C with the same rotational barrier energies, $\sigma = 0.43$ and $\omega = 0.035$. At this temperature, averages are higher and distribution functions are narrower since the chains become stiffer. The results for $F(\mathbf{R})$ in the region close to the initial unit are shown in Table III for $R_0 = 1$, 2, and 4 bond lengths, $N = 10$, and $\delta\phi = 0°$.

The model with long-range interactions gives averages of coordinates practically identical with those obtained with the simpler rotational isomeric model. This fact means that long-range interactions do not affect significantly the dimensions of the short chains studied in this work. Distribution functions are mainly affected by the interactions between the chain ends. If end-to-end steric effects are ignored so that only intramolecular interactions are taken into account, the values of $F(\rho_1,\rho_2,\rho_3)$ do not vary appreciably with respect to the rotational isomeric results. Nevertheless, there is a noticeable effect of the intramolecular long-range interactions on the probability densities around $R = 0$. Table IV shows the results obtained considering these interactions for $R_0 = 2$ and 4 bond lengths in a chain with $N = 10$ and $\delta\phi = 0°$ at 140 °C.

IV. Conclusions

Figures 1–6 allow us to compare the simulation results obtained here for $\delta\phi = 0°$ with results obtained with quasi-analytical methods and, therefore, ascertain the accuracy of the latter methods. The figures contain results obtained by Yoon and Flory[6] through a Hermitian series expansion of $F(\rho_1,\rho_2,\rho_3)$ in terms of these Cartesian coordinates.[15] We have also plotted values calculated in previous work[11] with the double-expansion method described in the Introduction. It is clearly shown that the double-expansion results agree much more closely with the simulation values than the Yoon and Flory estimates. Error ranges of the double-expansion results are, however, about 1×10^{-3} and 3×10^{-5} bond length for $N = 10$ and 20, respectively, i.e., about 3 times higher than those initially predicted.[11] Notwithstanding, we think that the double-expansion method can be considered accurate enough to describe qualitatively and quantitatively the behavior of the distribution function for these chains. Therefore, the conclusions previously obtained[11] about the shape of the functions and the lack of physical meaning of some features observed in the Yoon and Flory curves are fully confirmed. The remarkable differences between the results on axes ρ_2 and ρ_3, not observed in the Yoon and Flory values, are also verified, while the small oscillations of the double-expansion results are definitely attributed to truncation errors. The results for $\delta\phi = 15°$ contained in the figures present broader distribution in some cases, caused by the flexibility inherent to fluctuating rotational angles. However, as previously discussed,[11] the main features of the functions are not much affected by the fluctuations. Differences between quasi-analytic and simulation results are, of course, smaller for longer and more flexible chains.

From the values of the probability density around $R = 0$ shown in Tables I–IV we can establish some conclusions. As explained in the Introduction these values cannot be currently obtained by quasi-analytical methods. It can be observed that for $R_0 \leq 2$ bond lengths the probability density is noticeably higher in regions corresponding to positive values of x and negative values of z. For $R_0 > 2$ bond lengths the probability density is considerably smaller in regions where x and z are negative. These conclusions are general though they are more clearly manifested for stiffer chains, i.e., for decreasing values of temperature, N, and $\delta\phi$. (For $N = 20$, the chain is moderately flexible so that orientational correlations practically disappear, especially when rotational fluctuations are introduced.) Chains with intramolecular long-range corre-

lations follow the same behavior, though they present some interesting qualitative and quantitative differences. Thus it should be noted that these interactions affect more strongly the results as R_0 decreases so that for $R_0 = 1$ bond length and $N = 10$ the probability density becomes zero in all the octants.

The effect of rotational fluctuations on orientational preferences is manifested in a complex way. An increase of the chain flexibility causes a smoothing of these preferences coupled with an increase of the global probability density within the sphere. The fifth column of Table II, corresponding to a chain with $N = 15$ and $\delta\phi = 0°$, gives a value for the mean probability density within a sphere of radius $R_0 = 2$ bond lengths of 6.6×10^{-5} (bond length)$^{-3}$, smaller than $F(0)$, the value of $F(R)$ at $R = 0$, or the ring probability[9] 8.25×10^{-5} (bond length)$^{-3}$. This suggests that the sphere represents a very narrow fraction of the total volume available for the chain's last unit so that the probability density inside this region cannot be represented by a continuous distribution function and, in this case, is affected by a local fluctuation that yields an anomalously small value. Since local fluctuations should be very sensitive to changes in the chain model, it is not surprising that rotational fluctuations tend to increase dramatically the probability density in all the octants, while the decrease of orientational correlations seems to be a secondary effect.

On the other hand, the relative volume is higher for a sphere of the same radius in the case of a chain with $N = 10$. In fact, the fifth column of Table I shows a mean probability density within the sphere of 6.2×10^{-5} (bond length)$^{-3}$, which is considerably higher than any estimated value of the ring probability[9] for this chain with $\delta\phi = 0°$. Thus the mean probability density must represent an average over a relatively wide region. Therefore an increase in flexibility caused by rotational fluctuations tends mainly to smooth orientational preferences, as observed by comparing the results concerning this chain in Tables I and II.

A similar reasoning holds for the $N = 20$ chain. Although in this case the sphere with $R_0 = 2$ bond lengths represents a relatively narrow region (even narrower than that for $N = 15$), the remarkable flexibility of the chain gives a mean probability density slightly higher than the value of the ring probability,[9] 1.0×10^{-4} (bond length)$^{-3}$. Therefore rotational fluctuations are again mainly manifested through the smoothing of orientational preferences. Our conclusion is, consequently, that the rotational fluctuations exert a noticeable influence on the numerical results of the probability density in regions close to $R = 0$, though the description of this influence cannot be adequately accomplished unless a detailed balance of different factors is performed for every particular case.

We hope that the results obtained in regions close to $R = 0$ will help in understanding cyclization and intramolecular charge-transfer processes that are related to the conformational properties in these regions. Intramolecular charge-transfer reactions occur in flexible chains whose ends have been substituted by reactive groups[4,5] and, consequently, our conclusions may be useful when combined with considerations about the geometrical constraints imposed by particular end groups. These reactions seem to operate under conformational control, as it has been recently pointed out.[16]

References and Notes

(1) Flory, P. J. "Statistical Mechanics of Chain Molecules"; Wiley: New York, 1969.
(2) Yamakawa, H. "Modern Theory of Polymer Solutions"; Harper and Row: New York, 1971.
(3) Baram, A.; Gelbart, W. M. *J. Chem. Phys.* **1977**, *66*, 617.
(4) Sisido, M.; Shimada, K. *Macromolecules* **1979**, *12*, 790.
(5) Sisido, M.; Shimada, K. *Macromolecules* **1979**, *12*, 792.
(6) Yoon, D. Y.; Flory, P. J. *J. Chem. Phys.* **1974**, *61*, 5366.
(7) Fixman, M.; Alben, R. *J. Chem. Phys.* **1973**, *58*, 1553.
(8) Fixman, M.; Skolnick, J. *J. Chem. Phys.* **1976**, *65*, 1700.
(9) Freire, J.; Fixman, M. *J. Chem. Phys.* **1978**, *69*, 634.
(10) Fixman, M. *J. Chem. Phys.* **1973**, *58*, 1559.
(11) Freire, J. J.; Rodrigo, M. M. *J. Chem. Phys.* **1980**, *72*, 6376.
(12) Mansfield, M. L. *J. Chem. Phys.* **1980**, *72*, 3923.
(13) Cook, R.; Moon, M. *Macromolecules* **1980**, *13*, 1537.
(14) Freire, J. J.; Horta, A. *J. Chem. Phys.* **1976**, *65*, 4049.
(15) Flory, P. J.; Yoon, D. Y. *J. Chem. Phys.* **1974**, *61*, 5358.
(16) Winnik, M. A. *J. Am. Chem. Soc.* **1981**, *103*, 708.